Electrification of a bus system with fast charging stations
Impact of battery degradation on design decisions

Sharif Azadeh, Sh; Vester, J.; Maknoon, M. Y.

DOI
10.1016/j.trc.2022.103807

Publication date
2022

Document Version
Final published version

Published in
Transportation Research Part C: Emerging Technologies

Transportation Research Part C 142 (2022) 103807

Contents lists available at ScienceDirect

Transportation Research Part C

journal homepage: www.elsevier.com/locate/trc

Electrification of a bus system with fast charging stations: Impact of battery degradation on design decisions

Sh. Sharif Azadeh [a,b], J. Vester [a], M.Y. Maknoon [c,*]

[a] Econometric Department, Erasmus University Rotterdam, Netherlands
[b] Transport and Planning Department, Delft University of Technology, Netherlands
[c] Faculty of Technology, Policy, and Management, Delft University of Technology, Netherlands

ARTICLE INFO

Keywords:
Electrification of bus systems
Network design
Battery degradation
Charging policies
Mixed-integer linear problem

ABSTRACT

In this paper, we evaluate the cost of the electrification of an existing bus network. We propose a family of bi-objective mathematical models to demonstrate the trade-off between strategic (i.e., battery sizing and the locations of charging stations) and operational decisions (i.e., battery degradation). The proposed mathematical models investigate different charging policies and measure their impacts on overall cost. Battery degradation is estimated by a tailored and linearized semi-empirical approach and is explicitly incorporated in the proposed mixed-integer linear models. The impact of different charging policies on reducing the overall costs is evaluated for a bus network in Rotterdam. The results show that allowing for flexibility in the loss of energy levels at each bus cycle results in savings up to 17% in battery aging.

1. Introduction

The Netherlands is one of the most progressive EU countries when it comes to reducing CO2 emissions. In 2016, the Dutch government signed an agreement with all public transport providers requiring that, from 2030 onward, no diesel buses will be allowed to operate. As a result, public transport operators need to adapt the existing infrastructure to accommodate electric buses (see Waterstaat, 2016; Edenhofer, 2015). In recent years, several initiatives have taken place designed to incorporate Battery-powered Electric Bus (BEB) services in public transport systems (see Lajunen, 2014a; Li, 2016; Xu et al., 2016 and World, 2008).

While diesel buses can often run for an entire day without having to refuel, BEBs may need to be charged several times a day, limiting their capabilities to operate. To overcome this issue, there are three types of solutions for recharging BEBs: station-based charging, wireless lane-based charging and battery swapping (Li, 2016; Chen et al., 2017). In this research our focus is on electrification of a bus system with station-based charging. With the emerge of fast-charging technology, BEBs have the opportunity of being charged en-route while passengers board and alight. This technology enables BEBs to extend their service time. Their operation becomes similar to diesel buses and transport agencies can easily adapt them with their current timetable and vehicle scheduling plans (Augé, 2015).

On the other hand, the operation of BEBs also poses various strategic, tactical, and operational challenges (Scarinci et al., 2019) At a strategic level, the Public Transport Operator (PTO) needs to design its network's infrastructure by choosing the type and location of charging stations and the size of the bus batteries. The selected infrastructure has to be aligned with classical constraints, such as the PTO's network structure, schedule requirements, fleet size, and staffing considerations (Abdelwahed et al., 2020).

* Corresponding author.
E-mail addresses: s.sharifazadeh@tudelft.nl (Sh. Sharif Azadeh), jeroensvester@gmail.com (J. Vester), M.Y.Maknoon@tudelft.nl (M.Y. Maknoon).

https://doi.org/10.1016/j.trc.2022.103807
Received 29 November 2021; Received in revised form 8 July 2022; Accepted 10 July 2022
Available online 21 July 2022

The cost function for designing a network of electric buses can be formalized using two components: initial investment costs, and battery aging costs. Especially for the network of fast-charging BEBs, the battery lifetime plays a key role in the network design decisions, for cost-related reasons. According to Quarles et al. (2020), the average battery price for an electrical bus is estimated to be around $100,000, and that could be even higher for fast-charging buses with newer technologies. As a result, having more comprehensive network design models that explicitly take battery degradation into account could save the public transport operators substantial costs, given their large fleet sizes. However, estimating battery lifetime is difficult, due to their high dependency on operational factors like State-Of-Charge (SOC) and Depth-Of-Discharge (DOD), and temperature as direct consequences of infrastructural design decisions (Barré et al., 2013).

In literature, the electrification of a bus network is usually designed in one of the three following ways: (i) the location of charging stations is known and the model decides the size of the batteries, (e.g., Perrotta et al., 2014), (ii) battery capacities are given, and the model decides the location of the charging stations (e.g., Sebastiani et al., 2016,) and (iii) the proposed model decides both the battery sizes and the location of the charging stations (e.g., Kunith et al., 2017). Even though the cost of battery replacements is substantial, none of the above-mentioned researches takes battery degradation (i.e., battery aging) into account when determining the battery sizes, charging locations, or both, because of the computational burden of incorporating nonlinear and complex battery degradation estimation functions in the optimization models.

In this paper, we propose a family of bi-objective mathematical models to optimize and assess the overall costs of electrification of an existing bus network, with the aim of finding a trade-off between strategic decisions (i.e., battery sizing and the location and the power level of charging stations) and operational decisions (e.g., daily DOD and SOC variation of batteries). We estimate the battery degradation function by a tailored and linearized semi-empirical approach, (Hoke et al., 2011). This function is incorporated explicitly in the optimization model and contains three main contributing factors in relation to battery degradation: DOD, SOC, and temperature.

We evaluate our models using a bus line in Rotterdam and show that incorporating battery degradation can increase battery lifetime by 17% without increasing the initial investment. We also provide extensive results on assessing the impact of more conservative as opposed to more risky charging strategies on the overall cost. The outcomes show that allowing for flexibility in charging and discharging patterns can significantly reduce overall costs.

The remainder of this paper is organized as follows. In Section 2, we present a summary of relevant literature. We describe the characteristics and assumptions of the problem in Section 3, while the battery degradation estimation method is introduced in Section 4. In Section 5, we discuss the family of mathematical models used to design infrastructure and an iterative algorithm intended to solve the model is presented in Section 6. The computational results are presented in Section 7 and, discuss the conclusion and possible avenue for future research in Section 8.

2. Related literature

In the context of electric vehicles, the adaptation of road networks to accommodate charging stations have been extensively studied in the literature, see, Shen et al. (2019) for a comprehensive review. At strategic level, most studies focus on designing charging infrastructures by taking into account various factors such as uncertainty in driving range, demand variation and capacity of charging stations., see also, Lee and Han (2017), Kınay et al. (2021), He et al. (2013), Yıldız et al. (2019) and, Zhang et al. (2017), Xu et al. (2017) for public charging stations, Brandstätter et al. (2017), Bekli et al. (2021), Hua et al. (2019) for car-sharing systems. At operational level, most papers focus on developing models and algorithm to extend battery lifetime, see, Pelletier et al. (2018), Schoch et al. (2018), Adler and Mirchandani (2014), Xu et al. (2021).

In contrast to road transportation network, the electrification of a bus network involves tackling codependent problems at strategic and operational levels. Earlier studies have generally focused on one of these perspectives. Strategic level problems involve the locations and power levels of the charging stations (see Chen et al., 2018; Li, 2016; Mohamed et al., 2017; Abdelwahed et al., 2020), while operational level problems involve the development of charging strategies that determine where and how long a particular bus needs to be charged. The solution to operational problems can provide valuable insights and help estimate battery lifetime. In this paper, we address both the location of charging stations and the type of batteries. Meanwhile, operational decisions like State-Of-Charge (SOC) and Depth-Of-Discharge (DOD) are used as the variables of the model to incorporate battery degradation (i.e., aging) in strategic decisions.

2.1. Strategic level decisions

This section introduces different types of strategic level problems whose decision variables are associated with battery sizing and/or charging locations. The first group of studies on designing BEB networks assumes that the location of charging stations is known, while a decision has to be made about battery sizing (see Rios et al., 2014; Perrotta et al., 2014). For example, Sinhuber et al. (2012) estimate the batteries' energy consumption to decide about their sizes relative to the locations of the charging stations.

The second group of studies assumes that the battery types and capacities are known, and the decision to be made involves the locations of charging stations (see Sebastiani et al., 2016 and Xylia et al., 2017). An (2020) proposes a stochastic optimization model to simultaneously determine the location of charging stations and bus fleet size, while considering variations in charging demand. This paper assumes all batteries are large enough to cover at least one round trip. Lin et al. (2019) propose a multi-stage planning approach to electrify the bus network taking into account the power grid and demand evolution for electric buses over time. Yıldırım and Yıldız (2021) introduce a column generation approach to determine the optimal configuration of electric buses

taking into account multiple depots, battery sizing combined with the decision on recharging technologies. Paul and Yamada (2014) propose a model for the electrification of a bus network. The authors consider a fleet of BEBs whose battery sizes are known, and introduce an optimization model to maximize the number of trips the electric buses can make.

To further reduce the cost of electrifying the bus network, the last group uses both battery sizing and the location of charging stations as strategic decision variables. Compared to the categories mentioned above, there is a limited number of papers dedicated to this topic. Rogge et al. (2015) use the existing bus timetable to propose a two-stage optimization approach. In the first stage, they position one charging station at each terminus and then determine the battery size for each route in the second stage. Their proposed approach limits the location of charging stations relative to the terminus. By relaxing this assumption, Kunith et al. (2017) introduces a mixed-integer model to design the network by determining the location of charging stations and the size of batteries simultaneously. Pelletier et al. (2019) present a comprehensive optimization approach that determines the cost-effective transition solution from conventional to electric fleets. The model considers bus purchase cost, salvage value, operating cost, and the cost of charging stations. The model determined the fleet composition and required charging infrastructure for the transition period. In this paper, we also determine both battery sizes and charging locations. Below, we introduce the operational level decisions before highlighting our contributions compared to existing literature.

2.2. Operational level variables

As mentioned at the beginning of Section 2, operational level variables are associated with the factors contributing to battery degradation (i.e., aging) such as State-of-Charge (SOC) and Depth-Of-Discharge (DOD). The main challenge is how to estimate battery aging given these variables in an efficient and a reliable manner. For a BEB network at operational level problems, battery lifetime is in most cases either ignored or assumed to be defined parametrically. According to literature, there are three approaches to estimating battery degradation: (i) electrochemical, (ii) empirical, and (iii) semi-empirical methods (see Barré et al., 2013 and Pelletier et al., 2017).

The first group (electrochemical simulation models) evolves around the theories explaining the actual cause of degradation at a molecular level. They look to explain the degradation mechanisms based on the loss of lithium ions and other active materials. At a strategic planning level, one can only predict the battery's operating pattern, and such detailed information cannot be predicted precisely. As such, electrochemical simulation models have limited practicality to be incorporated into the decision-making process at a strategic level (Marano et al., 2009).

The second group (empirical models) use large empirical data sets to fit the lifetime functions. They predict the battery's lifetime through interpolation and extrapolation of test results and field data. The empirical models are designed to predict the impact of a particular factor on battery degradation. In reality, several factors affect the degradation process of batteries, limiting the practical applicability empirical models (see Xu, 2013 and Marano et al., 2009).

To overcome the shortages and challenges of the above-mentioned methods, the last group (semi-empirical methods) is proposed to model battery capacity degradation for battery life assessments (Xu et al., 2016). These methods combine theoretical and experimental observations to predict battery life, taking into account various factors that affect battery degradation. In case of not having experimental observations, the semi-empirical model can be fitted to the output of other battery degradation formulation. This feature makes them conceptually compatible with many degradation models. In recent years, these methods have been incorporated successfully in operational problems to estimate battery lifetime. Pelletier et al. (2018) use semi-empirical methods to include battery degradation in solving electric vehicle scheduling problems. Barco et al. (2017) use semi-empirical methods to determine the optimal routing and scheduling of electric vehicles in a case study in Colombia, while Arslan et al. (2015) use these methods to identify the minimum cost path for Plug-in Hybrid Electric Vehicles (PHEV).

2.3. Summary and contributions

In this paper, we introduce a bi-objective optimization model to design a BEB infrastructure for the electrification of an existing bus network. The decision variables are defined at a strategic level to determine battery sizes and charging station locations, as mentioned in Section 2.1. Operational variables like SOC and DOD are included in the model to estimate battery degradation, via the tailored semi-empirical function discussed in Section 2.2. In Section 3, we describe the framework of the problem and the components of the network under consideration, while the details of the battery degradation function are described in Section 4.

3. Problem description

In this study, we design a network of electric buses (by electrifying an existing bus network) to minimize overall costs. The cost function has two components: (i) initial investment (purchasing charging stations and buses) and (ii) costs related to battery degradation. In this section, we present the network and discuss its characteristics. Fig. 1 contains a schematic representation of bus line. We present the bus network as a set of lines (noted by $l \in L$). For line l, all buses start and end their journeys from/at the depot, connected to the terminal., represented by Terminal A in Fig. 1. The depot is always equipped with chargers for overnight charging and is not part of the decision. For each line, the fleet size and the frequencies are given. We define a set of charger station types, $t \in T$, and a set of stops, $s \in S$. For each line the set of stops are presented by S_l and $S = \cup_{l \in L} S_l$. If at stop $s \in S$, we decide to install a charger, then we have a charging station of type $t \in T$. As shown in Fig. 1, some stops, such as stop 2 and stop

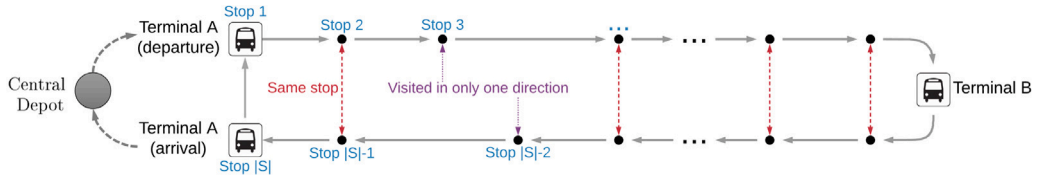

Fig. 1. A bus route model of circular bus line.

$|S|-1$, are shared between both directions. However, stops 3 and $|S|-2$ are only used in one direction. As mentioned, earlier, the model will not only decide on the location of the charging stations, but also the size of batteries.

Below, we discuss the components of the network and their associated definitions and characteristics.

Bus cycle. For a given line, the bus cycle is defined by a visiting order of stations, starting from the departure to the arrival point (e.g., Terminal A in Fig. 1). The bus's daily operations are presented by several bus cycles. For stop $s \in S$, we define parameter δ_s as the dwell time denoting the time planned for passengers' to board/alight. We also define parameter μ_s as the amount of energy required for a given bus to move from stop s to its successor. Between two stops, the energy consumption can vary during the day due to variations in travel demand and traffic congestion. However, we assume that these variations have a negligible impact on our point estimate.

We note that the operations of both circular and back-and-forth bus lines are presented by a bus cycle. This can be achieved by allowing stations to be visited in one or both directions. In this paper, a bus cycle shows one full trip of a given bus from a terminus to the same terminus. In this paper, *terminus* has a geographical meaning which shows the location at which a bus trip ends and *terminal* is an expression we use to show one of the types of charging stations. If a bus has a circular route, then each station is visited once. But, for a back-and-forth route, each station is visited at most twice. Fig. 1 illustrates the bus cycle for a circular line.

Charging stations. As suggested by Zanarini et al. (2020), we consider three types of charging stations. The first one is the so-called *Fast-Feeding Station* ($\mathscr{F}$), which provides fast charging at high power with the integrated energy storage system, making it possible to recharge a battery within 15 to 20 s, Augé (2015). An example to show the operations of these charging stations developed by ABB can be found in Infrastructure (2015)

The second one is called *Standard Feeding Station* ($\mathscr{S}$), which does not have an integrated storage system. Like $\mathscr{F}$, it is a fast-charging system but with a lower power and capacity. The last one is named *Terminal Feeding Station* ($\mathscr{T}$), that charges at a lower rate than $\mathscr{S}$. The set of charging stations then can be defined as $T = \{\mathscr{F}, \mathscr{S}, \mathscr{T}\}$. We need to indicate that the depot is different from a terminus, and it is always equipped with a charging station (not part of our decision-making process).

Battery. In this network, batteries have a modularized design that can be selected from a set of pre-defined configurations, presented by $i \in I$. For line l, we assume each bus performs a certain number of cycles. Therefore, all operated buses are assumed to be equipped with homogeneous batteries. As the depot is equipped with a charging station, we assume that batteries are fully charged at the beginning of each day. This assumption is motivated from the current practice and is not restrictive to our model. When a bus is connected to the *Fast-Feeding Station* ($\mathscr{F}$), it follows a *constant power–constant voltage* charging approach. According to this approach, the battery state-of-charge can be precisely approximated by a linear function up to 90% of the capacity of the battery (Tomaszewska et al., 2019). This is not the case for the remaining 10% (i.e., the battery requires more time to be fully charged). In this paper, Fast-Feeding stations are used to charge the batteries during bus dwell time which is relatively short. Therefore, we assume that the state-of-charge can be increased up to 90% of the battery capacity. Finally, the battery reaches the end of its life when its capacity is reduced to 80% of its initial nominal capacity. At this point, the battery has to be replaced.

Battery cycle. A *battery cycle* is defined as the elapsed time between two consecutive charges at charging stations. In Section 4, we provide details about the definition and estimation of battery degradation function.

4. Battery degradation estimation

Battery degradation is divided into two components, calendar aging and cycle aging. Calendar aging is the irreversible proportion of lost capacity during storage caused by battery storage conditions and is independent of the infrastructure design (Erdinc et al., 2009). Cycle aging, on the other hand, is associated with the impact of battery utilization periods called cycles (charge or discharge) during daily operations (Barré et al., 2013). In this paper, we are interested in estimating battery degradation resulting from cycle aging. This estimation function will be incorporated in our optimization framework involving the choice of the type and location of charging stations. This section presents a semi-empirical approach introduced earlier in Section 2.2 to estimate battery degradation.

We define $g^{cycle}(DOD, SOC, temp)$ as an estimation function to calculate relative lifetime loss of battery taking three degradation factors: (1) Depth-of-Discharge (g^{DOD}), (2) State-Of-Charge (g^{SOC}), and (3) the battery's temperature (g^{temp}) (Hoke et al., 2011). Each component of the g^{cycle} can be estimated separately using an empirical model. Empirical models can provide a reliable estimation

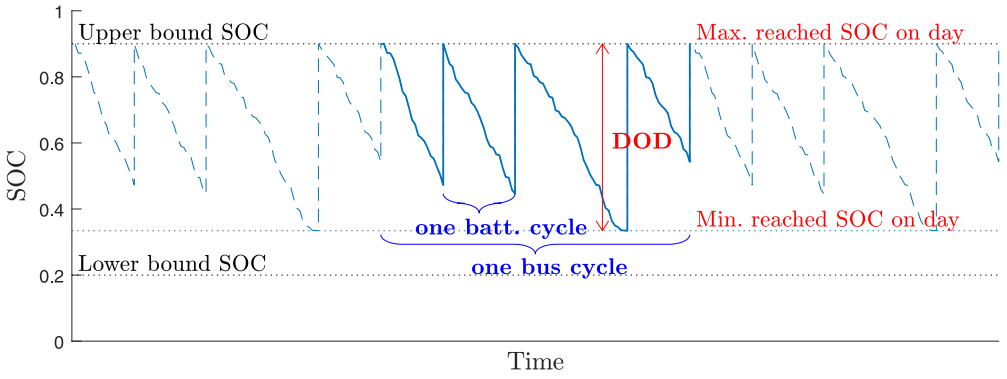

Fig. 2. Battery and bus cycles.

of the End-Of-Life (EOL) of batteries when experiments are conducted using new batteries. The reason is that the fitted distributions might not be as precise if used batteries are utilized to gather the data (Pesaran et al., 2009).

Estimation of relative battery lifetime. For each component of g^{cycle}, we estimate the degradation as a relative lifetime loss ($\frac{\Delta\mathcal{L}}{\mathcal{L}}$), in which $\mathcal{L}$ is the maximum estimated lifetime and $\Delta\mathcal{L}$ the actual lifetime under a given operating time interval. Eq. (1) shows the relationship between g^{DOD}, g^{SOC} and g^{temp}. Each one of these factors is estimated using an empirical method.

$$g^{cycle}(\cdot) = g^{DOD}(\cdot) + g^{SOC}(\cdot) + g^{temp}(\cdot) \tag{1}$$

These three degradation factors considered in Eq. (1) can cause amplifying effects on each other. In this paper we consider the above semi-empirical model proposed by Hoke et al. (2011) to model battery aging. Two assumptions facilitate the tractability of the model without jeopardizing its precision. (1) The effect of each degradation factor (i.e., $g^{DOD}(\cdot)$, $g^{SOC}(\cdot)$, $g^{temp}(\cdot)$) is assumed independent from other ones, and (2) these effects are assumed to be independent from battery's age (time-invariant over the battery lifetime). In Hoke et al. (2011), the authors show that despite imposed assumptions made in estimating battery lifetime, the outcome is compatible with the model proposed by NREL (The National Renewable Energy Laboratory). In Smith et al. (2010), the authors show that this semi-empirical model behaves similar to the physical data. In the following section, we explain these estimations separately.

4.1. Depth-Of-Discharge (DOD)

For each bus cycle, the Depth-Of-Discharge (DOD) is defined as the highest value of battery discharge over all battery cycles, as shown in Fig. 2, where the DOD represents the maximum usage of battery capacity at each bus cycle. Over all battery and bus cycles, the more frequently the battery's level reaches the maximum capacity usage, the higher its impact on the battery degradation will be. An empirical model that fits a distribution function over-collected data is used to estimate DOD per bus cycle.

To estimate the g^{DOD} in Eq. (1), we use the concept of *energy throughput* introduced by Marano et al. (2009), which is expressed as the expected amount of energy a battery can store and deliver. For a given battery cycle with the highest DOD (shown by $\overline{DOD}$) over all bus cycles, the energy throughput is calculated by $E_{cycle} = \overline{DOD} \times \kappa_i$ where $i \in I$ is the set of battery configurations and κ_i is capacity associated with the battery configuration i. As noted by Hoke et al. (2011), choosing the highest DOD will provide an accurate estimation. It also leads to a solution with a uniform charging/discharging pattern.

We also define the average depth-of-discharge over all battery cycles, presented by DOD^{avg}, used to estimate the number of cycles (N) that can be executed by the battery before reaching its EOL (The battery capacity is 80% of its initial nominal value). The battery manufacturing company provides this empirical information. Eq. (2), proposed by Hoke et al. (2011), is used to estimate the number of cycles.

$$N = \left(\frac{DOD^{avg}}{145.71}\right)^{\frac{-1}{0.6844}} \tag{2}$$

Given the information presented above, the total *energy throughput* over the battery lifetime is estimated as, $E_{total} = N \times DOD^{avg} \times \kappa_i$. Finally, the degradation function is estimated as follows,

$$g^{DOD} \approx \frac{\Delta\mathcal{L}_{DOD}}{\mathcal{L}} = \frac{E_{cycle}}{E_{total}} = \frac{\overline{DOD} \times \kappa_i}{N \times DOD_{avg} \times \kappa_i} \tag{3}$$

As N, $\overline{DOD}$ and DOD_{avg} are all variables, g^{DOD} is nonlinear. Eq. (3) also represents the relative battery lifetime loss resulting from the depth of discharge. For the sake of simplicity, we define $m = \frac{1}{N \times DOD_{avg}}$. Therefore, Eq. (3) can be replaced by $g^{DOD} = m\overline{DOD}$. Later, we present an iterative approach to deal with the nonlinearity of g^{DOD}.

4.2. State-Of-Charge (SOC)

The g^{SOC} function in Eq. (1) estimates the loss of battery lifetime resulting from the average State-Of-Charge (SOC), which in fact shows the range of charge level within which the bus operates, as shown in Fig. 2. We note that a smaller range of the SOC results in a smaller negative impact on the battery lifetime loss (see, Markel et al., 2009, Pesaran et al., 2009). Similar to g^{DOD}, the SOC function is estimated using an empirical method. In this paper, we consider the estimation for a given operating day. The relative lifetime loss of the battery associated with the SOC is presented as follows:

$$g^{SOC} \approx \frac{\Delta\mathcal{L}_{SOC}}{\mathcal{L}} = 24\left(\frac{0.4179 \cdot SOC^{avg} - 0.1685}{\zeta \cdot 15 \cdot 8760}\right) \tag{4}$$

According to Hoke et al. (2011), in Eq. (4), 0.4179 is the estimated slope of linear SOC degradation function and 0.1685 is its estimated intercept. In addition, ζ shows the maximum capacity fade at EOL of the battery. Finally, $\frac{\Delta\mathcal{L}_{SOC}}{\mathcal{L}}$ is estimated for an average of 15 years lifetime of the battery resulting in $15 \cdot 8760$ number of hours. As can be seen in this equation, a higher average SOC results in a higher relative battery lifetime loss. The average state of charge, SOC^{avg}, is affected by the location of the charging stations and the battery types. Later, we show how SOC^{avg} can be incorporated into our proposed family of MIP formulations.

4.3. Temperature

The last component in the $g^{cycle}(\cdot)$ function is presented by relative battery lifetime loss caused by the battery's temperature, represented by g^{temp}. The battery's temperature affects its lifetime, known as *temperature degradation*, which varies according to the rate at which the battery is charged or discharged. Here, we consider the degradation resulted from charging batteries. Longer and more frequent charging times increase the battery's temperature and consequently reduce its lifetime. The degradation resulting from discharging occurs independent from the design of the network therefore, it is left out of the degradation function.

We adapt the empirical model proposed by Hoke et al. (2011) to estimate the relative battery lifetime loss resulted from the battery temperature. In this model, one hour at temperature $Temp$ uses up a fractional lifetime $\frac{1}{8760\mathscr{L}(Temp)}$ in which the function $\mathscr{L}(Temp)$ shows the total number of years the battery would last at temperature $Temp$. Here, if the battery is charged at a station equipped with charger type $t \in T = \{\mathscr{F}, \mathscr{S}, \mathscr{T}\}$ then, $Temp = Temp_{amb} + R \cdot P^t$ in which $Temp_{amb}$ is the ambient temperature, R is the thermal resistance and P^t is the power of charger type t (kW). Similarly, if the battery is charged at the depot, the temperature is calculated by $Temp = Temp_{amb} + R \cdot P^{dep}$. In case, no charging is performed, the temperature is $Temp = Temp_{amb}$.

As the batteries have to be charged, we cannot avoid temperature-related degradation. Therefore, instead of considering the total degradation, we are interested in considering the degradation that could have been avoided. Based on the temperature function stated above, the minimum temperature while charging can be achieved when the charger has the minimum power. We assume that the charger installed at the depot has less power compare to the ones installed at the terminus and stops. At the depot, the charger with P^{dep} requires δ_{dep} hours to charge the battery. In this case, the baseline can be calculated as $\frac{\delta_{dep}}{8760 \cdot \mathcal{L}(Temp_{amb} + R \cdot P^{dep})}$.

To determine the degradation that could have been avoided, we determine the relative degradation if the battery is charged at terminus or stops. We already know that $\delta_s \leq \delta_{dep}$ as the chargers at the terminus or stops have more power than those at the depot. Therefore, we would like to estimate relative degradation if we have a dwell time of δ_{dep} to charge the battery. In this case the degradation is estimated as $\frac{\delta_s}{8760 \cdot \mathcal{L}(Temp_{amb} + R \cdot P^t)} + \frac{\delta_{dep} - \delta_s}{8760 \cdot \mathscr{L}(Temp_{amb})}$. Here the first term shows the degradation when the battery is charged at station s. The second term shows the degradation for the remaining time $(\delta_{dep} - \delta_s)$ in which the battery does not receive any charge.

By subtracting the baseline from the estimated degradation, for stop s and charger of type t, the temperature-related degradation can be estimated as

$$\frac{\Delta\mathcal{L}_s^t}{\mathcal{L}} = \underbrace{\frac{\delta_s}{8760 \cdot \mathscr{L}(Temp_{amb} + R \cdot P^t)}}_{\Delta\mathcal{L}/\mathcal{L} \text{ fast charging } t \in T} + \underbrace{\frac{\delta_{dep} - \delta_s}{8760 \cdot \mathscr{L}(Temp_{amb})}}_{\Delta\mathcal{L}/\mathcal{L} \text{ not charging at the depot}} - \underbrace{\frac{\delta_{dep}}{8760 \cdot \mathscr{L}(Temp_{amb} + R \cdot P^{dep})}}_{\Delta\mathcal{L}/\mathcal{L} \text{ slow charging at the depot}} \tag{5}$$

Here we have to note that δ_s is a parameter. For charging station type $\mathscr{F}$, the dwell time can be considered fixed. For other types of charging stations $(\mathscr{S}, \mathscr{T})$, the battery may require less time to be fully charged (reaching %90 of its SOC level). As the dwell times are short (less than 5 min), this has a negligible impact on the estimated value.

Knowing (5), the total degradation can be estimated by (6).

$$g^{temp} \approx \frac{\Delta\mathcal{L}_{temp}}{\mathcal{L}} = \sum_{t \in T} \sum_{s \in S} \frac{\Delta\mathcal{L}_s^t}{\mathcal{L}} \tag{6}$$

In contrast to the case involving DOD and SOC, estimated $\frac{\Delta\mathcal{L}_{temp}}{\mathcal{L}}$ is incorporated as a parameter in the proposed MIP models. In the section below, we introduce a family of mathematical models. The tailored semi-empirical approach to estimate the relative battery lifetime loss, presented in Eq. (1), is incorporated in all these models.

Table 1
Notations — sets and parameters.

Sets	
$l \in L$	Set of bus lines
$i \in I$	Set of pre-defined battery configuration
$t \in T$	Set of charger type $T = \{\mathscr{F}, \mathscr{S}, \mathscr{T}\}$
$s \in S_l$	Set of stops for line l
$s \in S$	Set of all bus stops
$s \in S^{\mathscr{T}}$	Set of terminus
$d \in D$	Set of stops whose charging stations can be potentially shared for both directions
$S_d \subseteq S$	Subset of stop pairs that can be location at $d \in D$
Parameters	
τ_{sl}	Travel time from stop s to its successor in line l
ν_{sl}	The required energy to reach the depot from stop s line l
μ_{sl}	Energy consumption between stops s and its successor in line l
δ_s	Dwell time at stop s
δ_{dep}	dwell time at the depot with its associated fixed charger type
β_l	fleet size for line l
κ_i	Capacity of battery configuration i
ω	Upper bound on the chargeable SOC
ζ	Maximum capacity fade at the End-Of-Life (EOL)
ϕ^t	Maximum charged energy at charging station type t
ρ_l	Number of cycles executed by a given bus per day, for line l
η_i	Battery lifetime under normal condition
$Temp_{amb}$	Ambient temperature
R	thermal resistance
P	Charging power (kW)
P^t	power of charger type t
P^{dep}	Power of charger at depot
Γ_i	Purchasing cost of battery i
γ_s^t	Cost of installing charging station type t at stop s
α_d^t	Cost saved when one charging station type t is installed at stop d that covers both directions
p^t	lifetime of charging station type $t \in T$

5. Family of mathematical models

In this section, we present three mathematical models to electrify an existing bus network. According to their associated charging policies, these models are distinguished from one another in ways that could result in different battery degradation costs. The aim is to minimize the total cost of both investment and battery aging.

The first model, called M1, assumes that all buses must be fully charged at the start of their cycle. The second model, M2, assumes that onboard batteries can lose a certain amount of energy in each bus cycle. In fact, M2 is a relaxation of M1. The energy loss involved is a decision variable in the model and it is the same for all bus cycles. At the end of a working day, the remaining energy on board should not drop below a predefined level. Finally, the last mathematical model, called M3, allows for a separate loss of energy level at each bus cycle resulting in a relaxation of model M2. Model M2 and M3 allow us to assess the impact of initial SOC and charging patterns on battery aging. The choice of charging policy represents the level of risk aversion and expected operational flexibility. For example, model M3 has limited flexibility to cope with unexpected events, including detours due to road closure and charging station failure. The introduction of these three charging policies enables public transport authorities to choose a design that meets their level of risk aversion. The summary of notations are reported in Tables 1 and 2.

5.1. Model M1: Full charge policy

The first proposed mathematical model (M1) can also be seen as the baseline model. In this problem, we assume that all buses must be fully charged at the beginning of each cycle. Therefore, no loss of energy level is allowed per cycle. We first present the mathematical model in its bi-objective form. The ϵ-constraint formulation is presented in objective function part. Defining $g^{cycle}(\cdot)$ as a function returning the battery degradation cost and g^{cost} as a function denoting the investment costs, the mathematical model to design the bus network is presented as follows:

$$\min \quad f(g^{cost}, g^{cycle}(\cdot)) \tag{7}$$

$$st.$$

(8)–(41)

Table 2
Notations — variables.

Variables	
$g_l^{cycle}(\cdot)$	Estimation function calculates lifetime loss of battery taking into account degradation factors, for line l
g_l^{DOD}	Relative lifetime loss of battery related to the Depth-of-Discharge (DOD) for line l
g_l^{SOC}	Relative lifetime loss of battery related to State-of-Charge (SOC), for line l
g^{temp}	Relative lifetime loss of battery related to temperature
N_l	Number of cycles, for line l
DOD_l^{avg}	Average depth-of-discharge over all battery cycle for line l
$\overline{DOD}_{il}$	Highest DOD of battery cycle for battery type $i \in I$
SOC_{il}^{avg}	Average state-of-charge for battery i
b_{il}	Binary variable equals to one if the battery configuration $i \in I$ is selected for line l
x_s^t	Binary variable taking value one if the charger type t is installed at stop s and zero, otherwise.
$x_d^{'t}$	Binary variable taking value one if the charger type t is installed at $d \in D$
z_{sl}	Energy level upon arrival of the bus at stop s, for line l
w_{sl}	The energy level upon departure from stop s for line l
y_{sl}	The amount of energy level charged at stop s for line l
h_{sl}^{dwell}	Represents the area underneath the SOC-graph during the bus dwell time for line l
h_{sl}^{travel}	Denote the area under the SOC-graph when bus moves from stop s to its successor for line l
o_l	Minimum energy level of the battery on board of the bus for line l
$\Delta_{cycle,l}$	Continuous variable show the difference in energy level between the starting and ending of each bus cycle.

The mathematical model has three blocks of constraints: (i) constraints related to the strategic variables (location and type of charging stations, and battery sizing), (ii) constraints related to the operational variables (e.g., SOC variation), and (iii) constraints related to the degradation. In the following parts, we first describe each block of constraints followed by the objective function.

Strategic variables and constraints. As mentioned in Section 3, for line $l \in L$ a bus cycle presents a certain order of bus stops $s \in S_l = \{1, 2, \dots, |S|\}$. Bus stop s can be shared with multiple bus lines. We denote the set of all bus stops by $S = \cup_{l \in L} S_l$. The bus stops show the potential locations for installing charging stations. We define the binary variable x_s^t with a value of one if charging type t is installed at stop $s \in S$, and zero otherwise. For line l, we assume that all buses are equipped with the same battery configuration chosen from the set $i \in I$. The binary variable b_{il} taking value one if the battery configuration $i \in I$ is selected for bus line l. Constraint (8) assures that only one battery type is selected and installed in all buses operating in the same line. At each stop s, one charging station $t \in T$ can be installed at the most, represented by Constraint (9). In this problem, in order to follow the existing conventional design, we assume that *Terminal Feeding Stations* ($\mathcal{T}$) are installed at the stops identified as terminus. Let $S^{\mathcal{T}} \subset S$ be the set of terminus, Constraints (10) enforce the model to install terminal feeding stations at the stops identified as terminus.

$$\sum_{i \in I} b_{il} = 1 \qquad \forall l \in L, \tag{8}$$

$$\sum_{t \in T} x_s^t \leq 1 \qquad \forall s \in S, \tag{9}$$

$$x_s^{\mathcal{T}} = 1 \qquad \forall s \in S^{\mathcal{T}}. \tag{10}$$

For a given bus cycle, a charging station can be used for both directions, as shown in Fig. 1 for stops 1 and $|S|-1$. We define $d \in D$ as the set of stops whose charging stations can be shared in both directions. As such, $S_d \subset S$ presents a subset of stop pairs that can be located at $d \in D$. Consequently, binary variable $x_d^{\prime t}$ indicates whether charging station type t is installed at $d \in D$. Constraints (11) show the relation between $x_d^{\prime t}$ and x_s^t. In other words, the purpose of this constraint is to take into account the potential cost saving (calculated in the objective) achieved by the economy of scale for the infrastructural construction.

$$x_d^{'t} \leq \frac{1}{2} \sum_{s \in S_d} x_s^t \qquad \forall t \in T, \forall d \in D \tag{11}$$

Operational variables and constraints. The second part of the constraints address the batteries energy level during the bus cycles. For line l, variable z_{sl} shows the energy level upon arrival at stop s, while variable w_{sl} shows the energy level upon departure from stop s. Finally, y_{sl} presents the amount of energy level at stop s. As mentioned in Section 3, μ_{sl} represents the energy consumption between two successive stops, i.e., s and its successor. Constraint (12) shows the energy level of the bus upon arrival at stop s. When the bus leaves stop s, the energy level of battery is equal to the energy level upon arrival plus the energy received at the charging

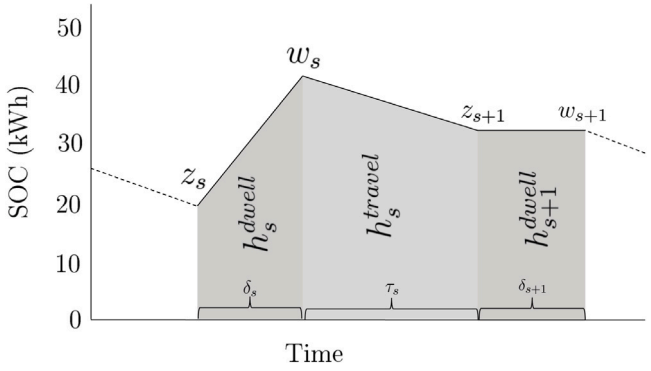

Fig. 3. SOC level for each pair of stops equipped with chargers to calculate the SOC_{avg}.

station, shown by Constraint (13).

$$z_{sl} = w_{s-1,l} - \mu_{s-1,l} \qquad \forall s \in S_l \setminus \{1\}, l \in L, \tag{12}$$

$$w_{sl} = z_{sl} + y_{sl} \qquad \forall s \in S_l, l \in L, \tag{13}$$

At stop s, if charging station of type $t \in T$ is installed, the amount of energy received by battery (y_{sl}) is calculated by $\min(\phi^t, \delta_s P^t)$ where ϕ^t is the maximum charged energy at charging station type t in kWh, δ_s shows the dwell time at stop s in seconds and P^t is the maximum power at station type t in kW. The above-mentioned relationship is formalized via the following constraints.

$$y_{sl} \le \sum_{t \in T} x_s^t \phi^t \qquad \forall s \in S_l, l \in L, \tag{14}$$

$$y_{sl} \le \sum_{t \in T} x_s^t \delta_s P^t \qquad \forall s \in S_l, l \in L, \tag{15}$$

During the operation, the SOC can vary within a given range, which is predefined by the operator. We previously introduced parameter κ_i as the capacity of battery configuration $i \in I$, and $b_i \in B$ as a binary variable equaling one if battery configuration i is selected. The lower bound on the SOC is shown by $\kappa_i \zeta$, where ζ is a proper number showing the maximum capacity fade at the battery's EOL. As discussed in Section 3, all chargers in the set T use a *constant power–constant voltage* charging approach, which means the battery cannot be fully charged and its charged level is bounded by $\kappa_i w$ where w is the upper bound (proper number) on the chargeable SOC. Constraint (16) guarantees the continuation of bus operation until the onboard battery of the bus reaches its EOL. Constraint (17) defines this upper bound for the battery charge. Constraint (18) assures that the battery onboard of the bus is fully charged at the beginning of the bus cycle.

$$z_{sl} \ge \sum_{i \in I} b_{il} \kappa_i \zeta \qquad \forall s \in S_l, l \in L, \tag{16}$$

$$w_{sl} \le \sum_{i \in I} b_{il} \kappa_i \omega \qquad \forall s \in S_l, l \in L \tag{17}$$

$$w_{1l} = \sum_{i \in I} b_{il} \kappa_i \omega \qquad l \in L, \tag{18}$$

Note that, based on our assumption, all buses start their first cycle with a fully charged battery. This assumption applies to all mathematical models proposed in this paper. Finally, to protect the bus operation in case of failure, all buses must maintain a minimum energy level to reach the depot. For stop s, we define ν_s as the required minimum energy to reach the depot. This condition is applied by Constraints (19).

$$w_{sl} \quad \ge \sum_{i \in I} b_{il} \kappa_i \zeta + \nu_{sl} \qquad \forall s \in S, l \in L, \tag{19}$$

Constraints related to battery degradation estimation. Constraints (20)–(23) are introduced to incorporate battery degradation behavior associated with the State-Of-Charge of batteries. More precisely, these constraints are used to calculate the average SOC (i.e., SOC_{avg} previously introduced in Section 4.2) that is used to calculate g^{SOC} in Eq. (4).

Fig. 3 presents the SOC level between a pair of stops. Here station s is equipped with a charger and no charger is installed at station $s+1$. To calculate the SOC_{avg}, we divide the area under the graph into two trapezoids. Constraints (20) and (21) calculate the average SOC for all stops except the depot for a given bus. The first trapezoid in Fig. 3 is associated with the bus's SOC level upon its arrival at stop s. If at stop s, we install a charging station, then the SOC level increases. The second trapezoid shows that the SOC level drops while traveling between stop s and $s+1$. The SOC_{avg} is calculated by summing up these two trapezoid areas.

We define an auxiliary variable associated with each trapezoid. For stop s in line l, variable h_{sl}^{dwell} represents the area underneath the SOC-graph during the bus dwell time. Given that each bus can on average perform ρ_l cycles per day, Constraint (20) shows how h_{sl}^{dwell} is calculated using z_{sl}, w_{sl} and δ_{sl}. Similarly variable h_{sl}^{travel} denotes the area under the SOC-graph when bus moves from stop s to its successor This value is calculated using w_{sl}, $z_{s+1,l}$, ρ_l and τ_{sl} shown by Constraint (21) that presents the travel time between the two stops. τ_{sl} is the travel time from stop s to its successor.

$$h_{sl}^{dwell} = \frac{1}{2}\rho_l(z_{sl} + w_{sl})\delta_s \qquad \forall s \in S, l \in L, \tag{20}$$

$$h_{sl}^{travel} = \frac{1}{2}\rho_l(w_{sl} + z_{s+1,l})\tau_{sl} \qquad \forall s \in S, l \in L, \tag{21}$$

Below, $v_{|S|,l}$ indicates the required energy to reach the depot from the last stop (noted by $|S|$) of line l. Constraint (22) calculates the average SOC of a given bus during its dwell time at the depot (δ_{dep} is the dwell time at the depot). Constraint (23) shows the average state-of-charge while traveling from the last station $|S|$ of line l to the depot. The travel time is noted by $\tau_{dep,l}$.

$$h_{dep,l}^{dwell} = \frac{1}{2}(\sum_{i\in I} b_{il}\kappa_i + w_{|S|,l} - v_{|S|,l})\delta_{dep,l} \qquad \forall l \in L, \tag{22}$$

$$h_{|S|,l}^{travel} = \frac{1}{2}(w_{|S|,l} + (w_{|S|,l} - v_{|S|,l}))\tau_{dep,l} \qquad \forall l \in L \tag{23}$$

The sum of all h-variables is equal to the area under the SOC-graph for a full day. We divide this sum by the battery capacity and the number of seconds (i.e., 86400) in a day, to determine the average SOC. Constraint (24) is used to determine the average SOC for battery configuration i. For line l, if battery $i \in I$ is selected (i.e., $b_{il} = 1$), the value of $SOC_{i,l}^{avg}$ will be equal to the calculated average SOC in the optimal solution. Otherwise, the right-hand side of the Constraints (24) will have a negative value and $SOC_{i,l}^{avg} = 0$ in the optimal solution. Note that, if $b_{il} = 0$, then the first term in the right-hand side of Constraints (24) is always greater than the second term.

$$b_{il} - SOC_{i,l}^{avg} \leq \tag{24}$$

$$\frac{\sum_{j\in I} b_{jl}\kappa_j}{\kappa_i} - \frac{\sum_{s\in S_l}\left[h_{sl}^{dwell} + h_{sl}^{travel}\right] + h_{dep,l}^{dwell} + h_{|S|,l}^{travel}}{86400\kappa_i} \qquad \forall i \in I, l \in L,$$

Constraints (25), estimates the degradation associated with SOC.

$$g_l^{SOC} = 24\left(\frac{0.4179\sum_{i\in I} SOC_{il}^{avg} - 0.1685}{\zeta \cdot 15 \cdot 8760}\right) \tag{25}$$

So far, we have estimated the average SOC used to calculate g_l^{SOC} as a component of battery degradation function g_l^{cycle}. Next, we aim to estimate the g_l^{DOD} function (another component of g_l^{cycle} or battery degradation function) by introducing Constraints (26) and (27). We define variable o_l to present the minimum energy level of the battery on board of the bus operate in line l. This value is bounded by z_{sl} (i.e, stored battery energy level upon arrival at stop s) as follows,

$$o_l \quad \leq z_{sl}. \qquad \forall s \in S_l, l \in L, \tag{26}$$

The depth-of-discharge for battery configuration i is presented by Constraint (27). Here, only one DOD_{il} variable assumes a positive value. The degradation associated by DOD is estimated by Constraint (28), in which $m = \frac{1}{N_l \times DOD_l^{avg}}$ as defined in Section 4.1.

$$DOD_{il} \geq b_{il} - \frac{o_l}{\kappa_i} \qquad \forall i \in I, l \in L, \tag{27}$$

$$g_l^{DOD} = m\sum_{i\in I}\overline{DOD_{il}}, \qquad \forall l \in L, \tag{28}$$

Finally, the degradation associated with the temperature is estimated by Constraint (29).

$$g^{tem} = \sum_{s\in S}\sum_{t\in T}\frac{\Delta L_{temp,s}^t}{L}x_s^t \tag{29}$$

Objective function: As mentioned earlier, the objective function is to minimize $f(g^{cost}, g^{cycle}(\cdot))$, in which g^{cost} shows the investment costs and $g^{cycle}(\cdot)$ the costs resulting from battery degradation. We present these two objectives in a linear fashion using the ϵ-constraints method. It is also possible to express the problem with a single objective function that translates all the cost values in monetary units. However, there are three main reasons for the choice of this bi-objective formulation: First, weighted-sum method only returns a single optimal solution. Whereas, with the $\varepsilon-$constraints method, one can generate the Pareto Frontier. With this frontier, we aim at providing a series of design solutions. Based on several post-processing techniques, practitioners could then decide which scenario is more suitable. Second, we study the problem at the strategic level when the time horizon is given. Battery lifetime is the output of our model. Therefore, battery cost is not fixed for the selected horizon (we may need one or several battery replacements). Incorporating these conditions will result in an intractable non-linear model. However, by choosing a given solution, one can easily convert the battery lifetime into a monetary value in a post-processing phase. Finally, explaining the problem as a single objective adds an extra layer of complexity to the solution, meaning that one needs to analyze the sensitivity (and stability

of the solution) based on the weights assigned to each objective. The investment costs (30) are a combination of battery purchasing cost and the cost of installing charging stations.

$$g^{cost} = \min \quad \sum_{l\in L}\sum_{i\in I}\beta_l \frac{\Gamma_i b_{il}}{\eta_i} + \sum_{t\in T}\left[\frac{\sum_{s\in S} x_s^t \Gamma_s^t - \sum_{d\in D} x_d^t \alpha_d^t}{p^t}\right] \tag{30}$$

For battery type $i \in I$, we let Γ_i be its purchasing cost and η_i is an upper bound for battery lifetime. Here, we have to note that we use η_i to normalize the purchasing cost of the battery. The first term in Eq. (30) shows the normalized purchasing cost where β_l is the fleet size. In the second part of the function (showing the investment costs in relation to infrastructure), Γ_s^t is introduced as the cost of installing charging station type t at stop s, and α_d^t presents the cost saved when one charging station type t is installed at stop d that covers both directions. Finally, p^t shows the lifetime of charging station type $t \in T$. The second objective in this problem has to do with limiting battery degradation, whose function is expressed by $g^{cycle(\cdot)}$ first introduced in Section 4. We express this objective by an ϵ-constraint shown in Constraint (31).

$$\epsilon_{deg} \geq \sum_{l\in L}\beta_l(g_l^{SOC} + g_l^{DOD}) + g^{temp} \tag{31}$$

Finally, the domain of variables are presented as follows.

$$x_s^t \in \{0,1\} \qquad \forall t \in T, \forall s \in S, \tag{32}$$

$$x_d^t \in \{0,1\} \qquad \forall t \in T, \forall d \in D, \tag{33}$$

$$b_{il} \in \{0,1\} \qquad \forall i \in I, l \in L, \tag{34}$$

$$y_{sl} \geq 0 \qquad \forall s \in S_l, l\ inL, \tag{35}$$

$$z_{sl} \geq 0 \qquad \forall s \in S_l, l \in L, \tag{36}$$

$$w_{sl} \geq 0 \qquad \forall s \in S_l, l \in L \tag{37}$$

$$o_l \geq 0 \qquad \forall l \in L, \tag{38}$$

$$h_{sl}^{travel}, h_{sl}^{dwell} \geq 0 \qquad \forall s \in S, l \in L, \tag{39}$$

$$DOD_{il} \geq 0 \qquad \forall i \in I, l \in L, \tag{40}$$

$$SOC_{il}^{avg} \geq 0 \qquad \forall i \in I, l \in L. \tag{41}$$

In the following section, we introduce the second model that suggests a different charging strategy to evaluate the impact on the overall costs.

5.2. Model M2: Same charging policy for all bus cycles

In Model M1, we assumed that the battery is fully charged at the start of each bus cycle, which could limit the opportunities to identifying a network configuration that allows for lower battery degradation (a with it, a more cost-efficient solution). This section presents additional constraints to the model shown in Section 5.1 to relax the full charge assumption. Here, we define a continuous variable $\Delta_{cycle,l}$ to show the difference in energy levels between the start and finish of each bus cycle.

$$\Delta_{cycle,l} = w_{1,l} - w_{|S|,l}, \tag{42}$$

Fig. 4 shows the battery SOC level during the operation if the SOC can be reduced by $\Delta_{cycle,l}$ at each bus cycle. By adding the term $(\rho_l - 1)\Delta_{cycle,l}$ to Constraints (16), (19) and (24) we are able to guarantee their validity at each bus cycle. Note that ρ_l is the number of cycles executed by a given bus per day. The modified constraints are presented as follows:

$$z_{sl} \geq \sum_{i\in I} b_{il}\kappa_i\zeta + (\rho_l - 1)\Delta_{cycle,l} \qquad \forall s \in S, l \in L, \tag{43}$$

$$w_{sl} \geq \sum_{i\in I} b_{il}\kappa_i\zeta + v_s + (\rho_l - 1)\Delta_{cycle,l} \qquad \forall s \in S, l \in L \tag{44}$$

$$o_l \leq z_{sl} - (\rho_l - 1)\Delta_{cycle,l} \qquad \forall s \in S, l \in L, \tag{45}$$

In addition, the constraints associated with the calculation of the SOC need to be adapted to account for the gradual decrease in battery energy level throughout the day. Constraints (22) and (23) are modified to calculate the area under the SOC graph at the depot. The revised constraints are presented below,

$$h_{dep,l}^{dwell} = \frac{1}{2}\Big(\sum_{i\in I} b_{il}\kappa_i + w_{|S|,l} - (\rho_l - 1)\Delta_{cycle,l} - v_{|S|,l}\Big)\delta_{dep,l} \tag{46}$$

$$h_{|S|,l}^{travel} = \frac{1}{2}(w_{|S|,l} + (w_{|S|,l} - v_{|S|,l}) - (\rho_l - 1)\Delta_{cycle,l})\tau_{dep,l} \tag{47}$$

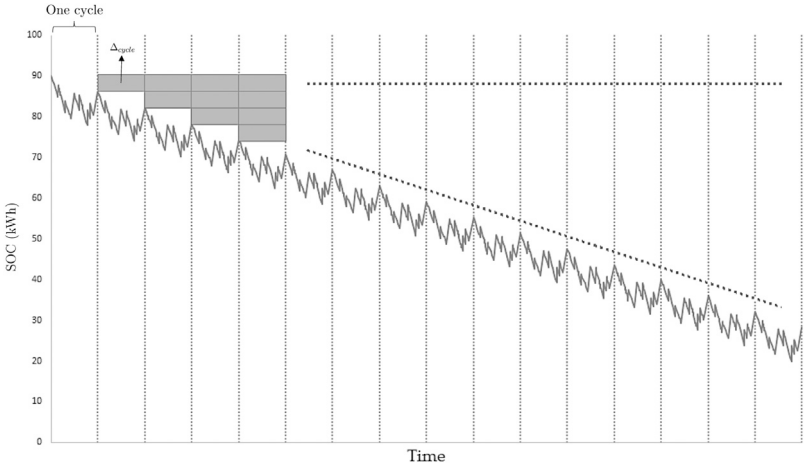

Fig. 4. Battery SOC level during operation considering Δ_{cycle}.

To calculate the average SOC, we define $\sum_{s\in S_l}\tau_{sl}$ as the total time it takes to complete a single bus cycle. For each bus cycle, the area underneath the SOC graph in Fig. 3 reduces with an area of $\Delta_{cycle,l}\sum_{s\in S_l}\tau_{sl}$. The sum of these excess areas must be subtracted from the sum of the h-variables. The total excess can be expressed as follows,

$$(1+2+3+\cdots+\rho_l-1)\Delta_{cycle,l}\sum_{s\in S_l}\tau_{sl}=\frac{1}{2}(\rho_l^2-\rho_l)\Delta_{cycle,l}\sum_{s\in S_l}\tau_{sl} \tag{48}$$

Finally, Constraint (24) is replaced by the following constraints,

$$b_{il}-SOC_{il}^{avg}\le\frac{\sum_{j\in I}b_{jl}\kappa_j}{\kappa_i}-\frac{\sum_{s\in S_l}\left[h_{sl}^{dwell}+h_{sl}^{travel}\right]-\frac{1}{2}(\rho_l^2-\rho_l)\Delta_{cycle,l}\sum_{s\in S_l}\tau_{sl}}{86400\kappa_i} \tag{49}$$
$$\forall i\in I, l\in L.$$

The remaining constraints are the same in model M1. The following section presents the final model that accounts for different charging policies at each bus cycle.

5.3. Model M3: Different charging policy for each bus cycle

Model M2 allows for battery energy reduction after each bus cycle. In Model M3, we evaluate the impact of allowing for different energy level losses after each bus cycle on the cost of battery degradation. In other words, M3 is the relaxation of M2. We further modify the M1 formulation to allow for variations in the SOC level during the day by duplicating bus stops for every bus cycle. To track the energy level status for each cycle separately, we define a new set $S'_l=\{1,\dots,|S|,|S|+1,\dots,2|S|,\dots,(\rho_l-1)|S|,\dots,\rho_l|S|\}$. To make sure that a charging station is installed at each duplicated stops, Constraint (50) is added to M1.

$$x_s^t=x_{s-|S|}^t,\qquad \forall t\in T,\forall s\in S'_l|s>|S|,l\in L, \tag{50}$$

The remaining constraints are similar to the ones presented in M1 and are adapted by using the set S'_l.

6. Linearization of degradation function

Models M1, M2, and M3 present three charging policies designed to charge an existing bus network. They all share the same objective function with two components. Investment costs are the main objective function, while battery degradation is presented as an ϵ-constraint, previously shown by Eqs. (30) and (31) (see Ngatchou et al., 2005 for an overview of ϵ-constraint methods). In this section, we present our approach to solving these proposed models.

First, we need to tackle the nonlinearity introduced by the degradation function, Eq. (1), in M1 to M3 models. In Section 5.1, we linearized $g^{SOC}(\cdot)$ function and incorporated its associated constraints in the model. The function g^{temp} is linearized with the help of enumeration. The only remaining source of nonlinearity is then the g_l^{DOD} function. In this section, we introduce an iterative approach to deal with this by solving a series of linear integer problems. Earlier, we presented a nonlinear empirical function $g_l^{DOD}=m\overline{DOD_i}$ to estimate the battery degradation caused by the depth-of-discharge for each type of battery. In Section 5.1, we presented Constraints (26) and (27) to calculate $\overline{DOD_i}$. Both m and $\overline{DOD_i}$ are variables that make g^{DOD} a nonlinear function.

The main idea behind our proposed iterative approach is to calculate the $\overline{DOD_i}$ for a given network configuration (including the decisions about the type of batteries and locations of charging locations) and to find its associated value of m_l. We first need to

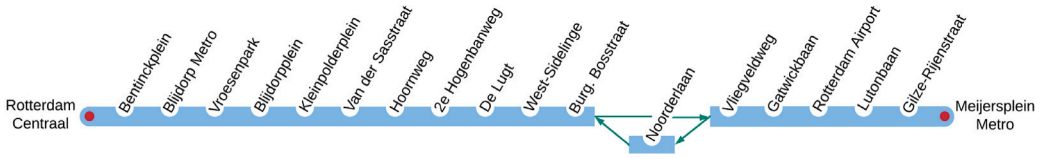

Fig. 5. Graphical depiction of all the stops on bus line 33.

calculate the DOD_l^{avg} that can be easily done for a given network design, after which the value of N is calculated by Eq. (2) and the degradation function g^{cycle} becomes linear.

Algorithm 1 presents the pseudocode of the iterative approach to solving M1, M2 and M3. We first define the notations applied in the algorithm. For a given charging policy M1, M2 or M3, we obtain an optimal solution called X^*. Estimated value of m_l is presented by $\hat{m}_l$ and $\hat{g}_l^{DOD}$ is the estimated value of g_l^{DOD}. Vector $\vec{X}^*$ contains all feasible solutions given different values of m_l, that satisfies the ϵ-constraint associated with the battery degradation.

In the first step of the algorithm, we set an initial value for $\hat{m}_l$. Then, we solve the MILP whose optimal solution is presented by X^*. Given the X^* and $\hat{m}_l$, we estimate the value of $\hat{g}_l^{DOD}$. By using the X^*, we obtain the actual value of m and consequently, g_l^{DOD} is calculated (steps 5 and 6). Then, we verify whether X^* is still feasible given the true value of g_l^{DOD} (i.e., feasibility condition: $g^{cycle} \leq \epsilon$). If this is the case, then we add X^* to the vector of feasible solutions, $\vec{X}^*$. We then update the value of $\hat{m}$ and repeat steps 3–9 till either $|\hat{g}_l^{DOD} - g_l^{DOD}| \leq \sigma_l$ where σ_l is a predefined small value or no new solution can be found. Finally, X^* (best solution) is obtained by finding the *argmin cost function* given the vector $\vec{X}^*$.

Algorithm 1: Iterative approach to solve models M_1, M_2 and M_3

Input: Model $M_j \quad j = 1, 2, 3$
DOD estimation function
Output: Best solution
1 Initialize $\hat{m}_l$
2 **do**
3 $X^* \leftarrow$ solve $M_j \quad j = 1, 2, 3$
4 $\hat{g}_l^{DOD} \leftarrow$ get DOD value $(X^*, \hat{m}_l, l)$.
5 $m_l \leftarrow$ get true $m_l(X^*)$
6 $g_l^{DOD} \leftarrow$ get DOD value (X^*, m, l)
7 **if** g^{cycle} *is infeasible with the new* g_l^{DOD} **then**
8 add X^* to $\vec{X}^*$.
9 **end**
10 $\hat{m}_l \leftarrow m_l$
11 **until** $|\hat{g}_l^{DOD} - g_l^{DOD}| \leq \sigma_l$ *for all* l *or no new solution can be found*;
12 $X^* \leftarrow$ argmin cost give $\vec{X}^*$

7. Computational results

In this section, we discuss the computational results. We apply our proposed models on bus line 33 in Rotterdam. We aim to evaluate the trade-off between the location of charging stations and their layout (i.e., number of charging stations, battery size, etc.) and battery degradation patterns. In fact, we investigate the benefit of applying different charging policies on battery lifetime. The details of our studied case are described in Section 7.1. In Section 7.2, we present the Pareto-frontier for models M1, M2, and M3. We discuss how the infrastructure design will evolve by varying the ϵ-value. We show that considering operational variables (e.g., SOC variation) can significantly reduce the investment cost. The benefits of integrating battery degradation in infrastructure design are discussed in Section 7.3. In Section 7.4 we present the extension of the results at the network level.

7.1. Case study description

We study the plan for the electrification of bus line 33, which moves between Rotterdam airport and the main train station. Figs. 5 and 6 present the locations of the various stations and the bus line that operates daily between 6 AM and midnight. Each round trip takes 51 min, and a fleet of 6 buses provides the service for this line. We assume that trips are distributed equally among these buses and that bus performs 16 cycles per day, i.e., $\rho_1 = 16$.

We use Google Maps to calculate the distances and travel times between each pair of stops assume that the dwell time at different stops adheres to a Normal distribution (expressed in seconds). For stops along the route, the dwell time is set by choosing a random number from $N(15, 5)$. The dwell time for terminals is chosen randomly from $N(210, 70)$. The dwell time at the terminal at the end of the bus cycle is defined such that the total duration of one cycle is exactly one hour. Finally, between each pair of stops, we calculate the consumed energy based on the approach proposed by Barco et al. (2017).

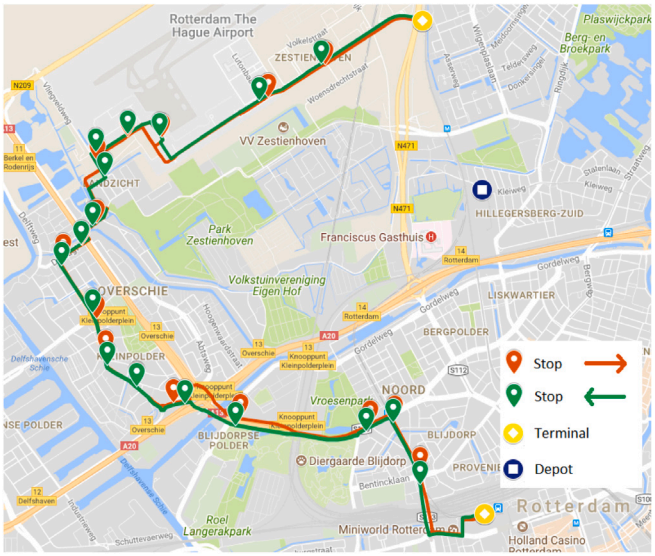

Fig. 6. Bus line 33 depicted on the map.

Table 3
Specification of charging stations.

Parameter description		Value	Unit	Ref.
Max. Power of stations	$P^{\overline{F}}$	600	kW	Pihlatie and Paakkinen (2017)
	$P^{\overline{S}}$	200	kW	Pihlatie and Paakkinen (2017)
	$P^{\overline{T}}$	100	kW	Pihlatie and Paakkinen (2017)
	P^{depot}	50	kW	Pihlatie and Paakkinen (2017)
Max. charged energy by stations	$\phi^{\overline{F}}$	10.00	kWh	Pihlatie and Paakkinen (2017)
	$\phi^{\overline{S}}$	2.0	kWh	Pihlatie and Paakkinen (2017)
	$\phi^{\overline{T}}$	5.0	kWh	Pihlatie and Paakkinen (2017)
Cost of installing charging stations	$\Gamma_s^{\overline{F}}$	200,000	€	Lajunen (2014b)
	$\Gamma_s^{\overline{S}}$	150,000	€	Lajunen (2014b)
	$\Gamma_s^{\overline{T}}$	120,000	€	Lajunen (2014b)
Savings of both ways installing charging stations	$\alpha_d^{\overline{F}}$	100,000	€	Lajunen (2014b)
	$\alpha_d^{\overline{S}}$	75,000	€	Lajunen (2014b)
	$\alpha_d^{\overline{S}}$	120,000	€	Lajunen (2014b)
Lifetime of charging stations	$p^{\overline{F}}$	4,380	days	Lajunen (2014b)
	$p^{\overline{S}}$	4,380	days	Lajunen (2014b)
	$p^{\overline{T}}$	4,380	days	Lajunen (2014b)

Table 3 presents the specification of charging stations. We use the information provided by Pihlatie and Paakkinen (2017) to determine the maximum power of charging station type t as well as the maximum charged energy, ϕ^t at station type t. The rest of the required information including Γ_s^t, α_s^t and p^t is obtained from (Lajunen, 2014b).

Parameters associated with batteries are presented in Table 4. Parameters related to the state-of-charge and the depth-of-discharge are borrowed from Hoke et al. (2011), while parameters associated with the temperature component of the degradation function are obtained from Barco et al. (2017).

7.2. Infrastructure design and charging policies

In this section, we discuss the computational results of our proposed models to evaluate the impact of different charging policies on battery degradation and overall costs. We implement Algorithm 1 in Java and use CPLEX 12.9 to solve the optimization problems. These models are solved on a computer with a 3.5 GHz processor and 16 GB RAM. All models can be solved in less than one hour. No significant difference have been observed by using different epsilon value. We present the Pareto frontiers for model M1, M2 and M3 in Fig. 7.

The costs of installing charging stations, battery costs and battery lifetime (in days) are presented in Figs. 7(a), 7(c) and 7(e). The change of infrastructure cost under different ε-values as well as the estimated achieved lifetime of batteries for each model are presented in Figs. 7(b), 7(d) and 7(f).

Table 4
List of parameters related to batteries.

Parameter description		Value	Unit	Ref.
Ambient Temp.	$Temp_{amb}$	25	^oC	Hoke et al. (2011)
Thermal resistance	R	4.10^{-5}	C/W	Hoke et al. (2011)
LB on the usable SOC	ζ	0.20		Assumptions
UB on chargeable SOC	ω	0.90		Assumptions
Cap. of bat. conf. $i \in I = \{1, \ldots, 16\}$	κ_i	$5i$	kWh	Assumptions
Marginal cost of battery	Γ_i	1000	€/kWh	Lajunen (2014b)
Upper bound for Battery lifetime	η_i	3,650	days	Lajunen (2014b)

The total investment cost and battery lifetime have opposite relationships. By imposing lower ε-values, i.e., a longer lifetime for battery, each model first tends to find a solution with a larger onboard battery (the battery cost increased by reducing the ε-values in Figs. 7(a), 7(c) and 7(e)). Then, by further decreasing the value of ε, it is more beneficial to add the number of charging stations resulting in higher investment cost. As can be seen in Figs. 7(a), 7(c) and 7(e), the station cost remains constant while ε-value decreases. In our case, the smallest ε-value in which a solution is found 1.4×10^{-3} equivalent to the lifetime of approximately 4500 days.

Comparing the solutions of the model M1 (full charge policy) and M2 (same charging policy for all bus cycles), we identify two patterns by varying allowed degradation. For $\varepsilon \geq 1.85 \times 10^{-3}$, we observe that relaxing the full-charge policy allows us to identify a network design with fewer charging stations (the station costs of the solutions reported in M2 is less than M1). Therefore, larger onboard batteries are installed while the total costs are reduced (higher battery cost). For smaller values of ε, both M1 and M2 find similar solutions in terms of the number of stations and battery sizes.

Model M3 (which imposes different charging policies for each bus cycle), on the other hand, finds solutions with the same number of stations as M2, but with smaller on board batteries for all values of ε. This result shows the significance of optimizing the charging policy at a strategic level. We note that although the solution of model M3 provides a solution with a minimum degradation, most of the time, it may also be less flexible while coping with unexpected events (e.g., detour due to construction, failure of charging stations, etc.). Therefore, careful examinations are required to choose one of the designs provided by M1, M2, and M3.

7.3. Benefits of including battery degradation on infrastructural design

In this section, we discuss the benefits of incorporating battery degradation when designing the BEBs infrastructure. We compare the solutions of the proposed M1, M2, and M3 models with their associated mathematical models (called O1, O2, and O3) in which battery degradation is not incorporated into the design decisions.

Table 5 summarizes the comparative results for our case study presented in Section 7.1. For M1, M2, and M3, we group the solutions with similar characteristics based on the number of stations and battery sizes. For the non-similar ones, we provide the range of solution values. The column called "class of solutions" presents the network configuration associated with the obtained solutions. The group of solutions are called A, B, C and D. Column ε-value report the imposed ε value. For each solution, the information about the batteries and charging stations are reported under the columns "Battery size", "Battery lifetime", and "Charging facilities". Finally column under "Station costs" reports the cost associated with the installation of charging stations.

By comparing the outcome of the different models, including and excluding battery degradation, we see that for a similar design (i.e., same battery size, number of stations, and costs), our proposed models (M1, M2, and M3 models) manage to improve battery lifetime. The corresponding rows in Table 5 are summarized in Table 6. Here, we compare the design obtained by models O_1, O_2 and O_3 with the one obtained by corresponding M_j model. Among the Pareto solutions resulting from models M_j, we choose the one which has the same design as model O_j (i.e., in terms of the number of charging stations, battery size and investment costs). The results show that incorporating battery degradation in designing the network of BEBs leads to significant improvements in battery lifetimes (%5, %15, and %17 for M1. M2 and M3, respectively) without increasing investment costs. Although both models use the same infrastructure. Models M_j positioned them in a way that increases battery lifetime, which is not the case for models O_j. From an economic perspective, these savings can be translated to 0.77%—4.74% of total investment cost, depending on the charging policy.

Finally, we investigate the relationship between battery lifetime and battery sizes for solutions with a similar number of charging stations. The corresponding Pareto solutions are summarized in Table 7. The first row shows the benchmark case when no battery degradation is incorporated into the objective function, but we allow for different charging policies. In the subsequent rows, we gradually increase the size of batteries proportional to the benchmark case.

For each model, three solutions are presented. The first group of solutions has a slightly larger battery size (i.e., less than two times the battery size in the benchmark solution). The second group has a larger battery size (more than two times larger than the benchmark), while the third group has slightly higher station costs (one additional station is installed). This shows that if the battery size increases by 50% its lifetime will also increase by the same amount. More than doubling the battery size causes the battery life

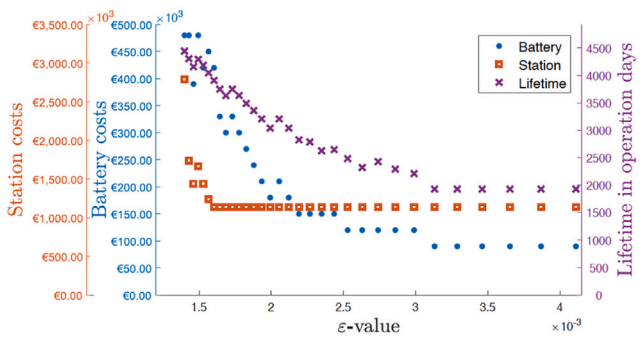

(a) Pareto Frontier M1

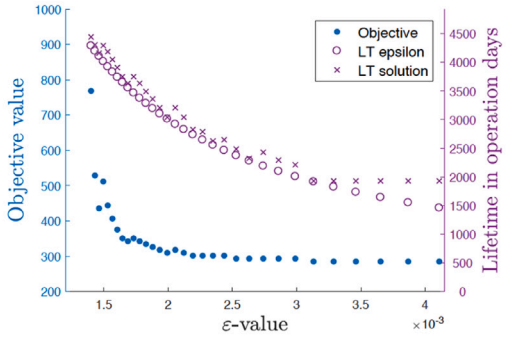

(b) Battery lifetime evaluation M1

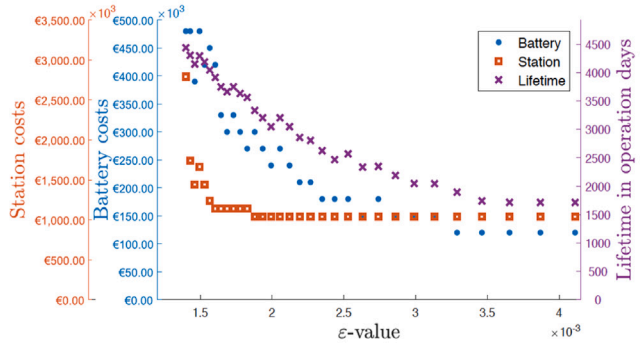

(c) Pareto Frontier M2

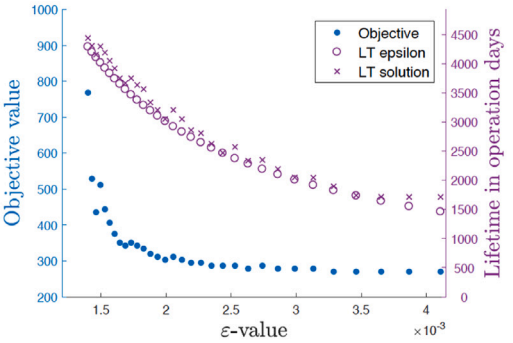

(d) Battery lifetime evaluation M2

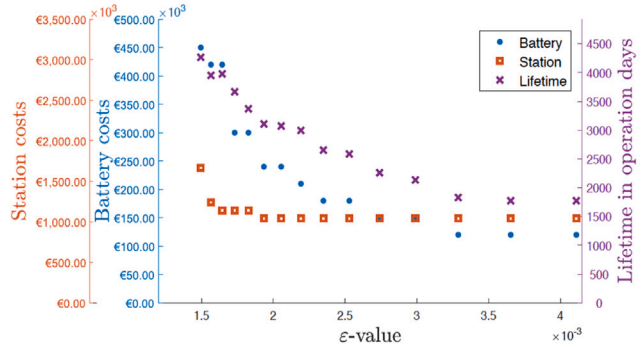

(e) Pareto Frontier M3

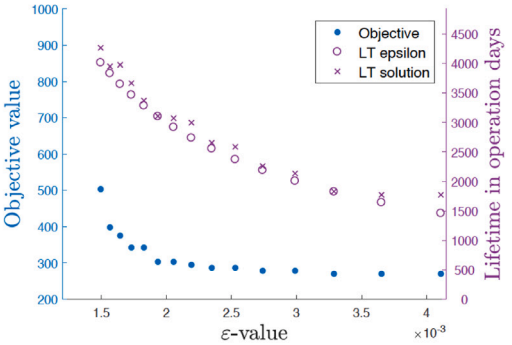

(f) Battery lifetime evaluation M3

Fig. 7. Pareto frontiers for the ϵ-constraint bi-objective models M1, M2 and M3.

to increase between 66% to 94%, and combining this with the installment of an extra station improves the results between 105% to 118%. These are cost-efficient solutions compared to the benchmark depending on the costs related to stations and the marginal costs involved in increasing the fleet's battery size.

7.4. Bus network

The previous sections discuss the impact of charging policies on infrastructure design and the benefit of considering battery degradation while designing infrastructure. This section investigates the changes in infrastructure design (i.e., type and the number of charging stations and battery sizes) when bus lines have partially shared stops.

We extend the single line network to create a network of two lines hub-and-spoke structure in which both lines start their trip from the central depot. Both lines share the same characteristics in terms of the number of stops, energy consumption between each

Table 5
Solution comparison between models excluding battery degradation (O1, O2, and O3) and the solutions of the Pareto-frontier obtained by models M1, M2, M3.

Model	Class of solutions		ϵ	Battery	Battery	Charging facilities		Station costs
	Name	Description	value	size (kWh)	lifetime (days)	$\#\mathcal{F}$	$\#\mathcal{S}$	€
O1			–	15	1835	6	0	1,140,000
M1	A	Same station costs, small battery	4.11E−03 ⋮ 1.88E−03	15 ⋮ 40	1929 ⋮ 3360	6	0	1,140,000
	B	Same station costs, large battery	1.83E−03 ⋮ 1.60E−03	45 ⋮ 70	3490 ⋮ 3909	6	0	1,140,000
	C	Large battery, increasing station costs	1.57E−03 ⋮ 1.43E−03	75 ⋮ 80	4047 ⋮ 4305	6 ⋮ 10	0	1,240,000 1,740,000
	D		1.40E−03	80	4442	16	1	2,790,000
O2				20	1458	5	0	1,040,000
M2	A	Same station costs, small battery	4.11E−03 ⋮ 1.88E−03	20 ⋮ 50	1713 ⋮ 3335	5	0	1,040,000
	B	Same station costs, large battery	1.83E−03 ⋮ 1.60E−03	45 ⋮ 70	3564 ⋮ 3916	6	0	1,140,000
	C	Large battery, increasing station costs	1.57E−03 ⋮ 1.43E−03	75 ⋮ 80	4047 ⋮ 4306	6 ⋮ 10	0	1,240,000 ⋮ 1,740,000
	D		1.40E−03	80	4439	15	1	2,790,000
O3				20	1479	5	0	1,040,000
M3	A	Same station costs, small battery	4.11E−03 ⋮ 1.93E−03	20 ⋮ 40	1774 ⋮ 3108	5	0	1,040,000
	B	Same station costs, large battery	1.83E−03 ⋮ 1.64E−03	50 ⋮ 70	3371 ⋮ 3978	6	0	1,140,000
	C		1.57E−03	70	3952	6	0	1,240,000
	D		1.49E−03	75	4267	10	0	1,740,000

Table 6
Comparison between battery lifetime gains when including and excluding degradation.

Model number		1	2	3
Battery lifetime (in days)	O	1835	1458	1479
	M	1929	1713	1774
Difference (days)		94	255	295
Imp. (%)		4.87	14.81	16.53
Battery cost per day (€)	O	49.05	82.30	81.14
	M	46.66	70.05	67.64
Battery cost planning horizon (€)	O	179019.07	300411.52	296146.04
	M	170295.49	255691.77	246899.66
Difference (€)		8723.58	44719.75	49246.38
(%) of investment cost		0.77%	4.30%	4.74%

pair of stops, and so on. We then define nine case scenarios for this extended two line network based on the bus frequencies and the percentage of shared stops (except the depot) across the network between two lines.

The descriptions of these networks are described in Table 8 and their associated schematic representations are shown in Fig. 8. The generated instances are categorized into three groups. In the first group (N1–N3), bus lines have no shared stops (except the central depot). In the second group, the first six stops are shared between two bus lines (N4–N6). Finally, in the third group (N7–N9), the first 12 stops of the bus lines are shared. Within each group, one bus line always performs 16 cycles per day, and the other one runs 16, 24, and 32 cycles. Note that bus bunching is not considered in the presented model.

We use model M3 to design the infrastructure. In order to have a fair comparison between instances, we only accept the solutions in which the battery lifetime is within the range (3500 – 4000) days and report the solution with the highest battery lifetime. The results of our experiments are shown in Table 9. For each network scenario, columns under "charging facilities" report the type

Table 7
Achieved improvement in battery lifetime when larger batteries are installed. Three solutions are presented for every model. The increase in costs, battery size and battery lifetime is compared to its associated benchmark model O_i, $i = 1, 2, 3$. The increase in station costs is 0% for the solutions where it is omitted.

Solution			Charging policy		
Class	Description		1	2	3
	Benchmark	Battery size	15 kWh	20 kWh	20 kWh
	Model O_i	Lifetime (days)	1835	1458	1479
A	**Input:**	Battery size	×1.7(25 kWh)	×1.5(30 kWh)	×1.5(30 kWh)
	Model M_i:				
	increase in :	Lifetime (days)	54%(2827)	80%(2625)	80%(2655)
A	**Input:**	Battery size	×2.3(35 kWh)	×2.5(50 kWh)	×2.0(40 kWh)
	Model M_i:				
	increase in :	Lifetime (days)	74%(3207)	128%(3335)	49%(3108)
C,B	**Input:**	Battery size	5.0(75 Wh)	×2.8(55 kWh)	×2.5(50 kWh)
	Model M_i:				
	increase in:	Station cost	8.77%	9.62%	9.62%
	increase in:	Lifetime (days)	120%(4047)	157%(3749)	76%(3667)

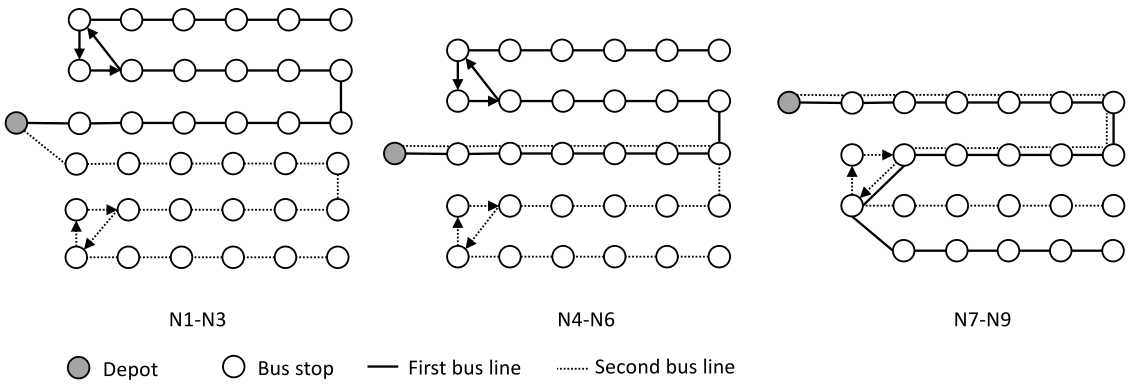

Fig. 8. Schematic representation of the networks.

Table 8
Characteristics of the generated scenarios.

	Instance name								
	N1	N2	N3	N4	N5	N6	N7	N8	N9
Shared stops	0	0	0	6	6	6	12	12	12
ρ_1	16	16	16	16	16	16	16	16	16
ρ_2	16	24	32	16	24	32	16	24	32

of charging stations, the number of shared charging stations, and the total number of installed charging stations. The battery size selected for each bus line is reported under the column "Battery size".

Instance N1 shows a bus network with two independent bus lines, which we use as a benchmark to compare other instances. For N1, the model results in an identical infrastructure design. This outcome is expected as both lines have similar characteristics. When the number of shared stops increases (instances N4 and N7), the model proposes the same number of charging stations with a slight modification on their positions. In these cases, the battery capacity remains the same. On the other hand, as bus lines contain shared bus stops, the total number of installed charging stations decreases. By increasing the number of cycles, the model increases the size of batteries and the number of charging stations for the second line. However, when they share several stops, the model suggests to install terminal feeding station shared between two lines.

8. Conclusion

In this paper, we examine the electrification of an existing bus line and proposed a family of mathematical models to make network design decisions related to the location of charging stations, their power type and battery sizing, while taking the costs of battery degradation into account. We used a semi-empirical approach to estimate battery degradation and incorporated it into the mathematical models. We presented a bi-objective approach, in which the first objective counts for the investment cost and the second objective estimates the battery degradation (formulated as ε-constraints).

Table 9
Design decisions for each network.

Name	Charging facilities						Battery size (kWh)	
	L_1		L_2				L_1	L_2
	$\#\mathcal{F}$	$\#\mathcal{S}$	$\#\mathcal{F}$	$\#\mathcal{S}$	Shared	Total		
N1	6	0	6	0	0	12	55	55
N2	6	0	7	0	0	13	55	60
N3	6	0	8	0	0	14	60	65
N4	6	0	6	0	3	9	55	55
N5	6	1	6	1	4	10	55	65
N6	5	2	7	2	4	12	65	70
N7	6	0	6	0	4	8	55	55
N8	6	2	8	2	6	12	60	70
N9	5	3	6	3	7	10	65	70

We applied our models to a bus line in Rotterdam and showed that incorporating battery degradation into the design process can significantly increase battery lifetimes without increasing the investment costs. Moreover, our results indicate that we can extend the battery lifetime by allowing flexibility in the charging/discharging policy. In this research, we assume that the BEBs operate in a deterministic environment. Although that assumption can provide realistic estimations in a number cases, it may not be suitable for bus networks with high demand fluctuations, because the energy being consumed can vary significantly during the day, resulting in reduced battery lifetimes. As an extension to the current research, we are interested in addressing uncertainties related to energy consumption in the design decisions. Our models can be extended to incorporate uncertainties in energy consumption using stochastic or robust optimization methods.

CRediT authorship contribution statement

Sh. Sharif Azadeh: Conceptualization, Methodology, Writing –original draft, Writing – review & editing. **J. Vester:** Methodology, Data curation, Software, visualization. **M.Y. Maknoon:** Conceptualization, Writing – review & editing, Software, Visualization, Methodology.

Appendix. Model M3

$$\min \quad \sum_{l\in L}\sum_{i\in I}\beta_l\frac{\Gamma_i b_{il}}{\eta_i}+\sum_{t\in T}\left[\frac{\sum_{s\in S}x_s^t\Gamma_s^t-\sum_{d\in D}x_d^t\alpha_d^t}{p^t}\right] \tag{A.1}$$

$$\epsilon_{deg}\geq\sum_{l\in L}\beta_l(g_l^{SOC}+g_l^{DOD})+g^{temp} \tag{A.2}$$

$$\sum_{i\in I}b_{il}=1 \qquad \forall l\in L, \tag{A.3}$$

$$\sum_{t\in T}x_s^t\leq 1 \qquad \forall s\in S, \tag{A.4}$$

$$x_s^{\mathcal{T}}=1 \qquad \forall s\in S^{\mathcal{T}}, \tag{A.5}$$

$$x_d'^t\leq\frac{1}{2}\sum_{s\in S_d}x_s^t \qquad \forall t\in T,\ \forall d\in D, \tag{A.6}$$

$$z_{sl}=w_{s-1,l}-\mu_{s-1,l} \qquad \forall s\in S_l'\setminus\{1\}, l\in L, \tag{A.7}$$

$$w_{sl}=z_{sl}+y_{sl} \qquad \forall s\in S_l', l\in L, \tag{A.8}$$

$$y_{sl}\leq\sum_{t\in T}x_s^t\phi^t \qquad \forall s\in S_l', l\in L, \tag{A.9}$$

$$y_{sl}\leq\sum_{t\in T}x_s^t\delta_s P^t \qquad \forall s\in S_l', l\in L, \tag{A.10}$$

$$z_{sl}\geq\sum_{i\in I}b_{il}\kappa_i\zeta \qquad \forall s\in S_l', l\in L, \tag{A.11}$$

$$w_{sl}\leq\sum_{i\in I}b_{il}\kappa_i\omega \qquad \forall s\in S_l', l\in L, \tag{A.12}$$

$$w_{1l}=\sum_{i\in I}b_{il}\kappa_i\omega \qquad l\in L, \tag{A.13}$$

$$w_{sl}\geq\sum_{i\in I}b_{il}\kappa_i\zeta+\nu_s \qquad \forall s\in S_l', l\in L, \tag{A.14}$$

$$x_s^t = x_{s-|S|}^t, \qquad \forall t \in T, \forall s \in S_l' | s > |S|, l \in L, \tag{A.15}$$

$$h_{sl}^{dwell} = \frac{1}{2}(z_{sl} + w_{sl})\delta_s \qquad \forall s \in S_l', l \in L, \tag{A.16}$$

$$h_{sl}^{travel} = \frac{1}{2}(w_{sl} + z_{s+1,l})\tau_{sl} \qquad \forall s \in S_l', l \in L, \tag{A.17}$$

$$h_{dep,l}^{dwell} = \frac{1}{2}(\sum_{i \in I} b_{il}\kappa_i + w_{|S|,l} - v_{|S|,l})\delta_{dep,l} \qquad \forall l \in L, \tag{A.18}$$

$$h_{|S|,l}^{travel} = \frac{1}{2}(w_{|S|,l} + (w_{|S|,l} - v_{|S|,l}))\tau_{dep,l} \qquad \forall l \in L \tag{A.19}$$

$$b_{il} - SOC_{i,l}^{avg} \leq \tag{A.20}$$

$$\frac{\sum_{j \in I} b_{jl}\kappa_j}{\kappa_i} - \frac{\sum_{s \in S_l}\left[h_{sl}^{dwell} + h_{sl}^{travel}\right] + h_{dep,l}^{dwell} + h_{|S|,l}^{travel}}{86400\kappa_i} \qquad \forall i \in I, l \in L,$$

$$o_l \leq z_{sl}. \qquad \forall s \in S_l', l \in L, \tag{A.21}$$

$$DOD_{il} \geq b_{il} - \frac{o_l}{\kappa_i} \qquad \forall i \in I, l \in L, \tag{A.22}$$

$$g_l^{DOD} = m \sum_{i \in I} \overline{DOD_{il}}, \qquad \forall l \in L, \tag{A.23}$$

$$g^{tem} = \sum_{s \in S}\sum_{t \in T} \frac{\Delta L_{temp,s}^t}{L} x_s^t \tag{A.24}$$

$$x_s^t \in \{0,1\} \qquad \forall t \in T, \forall s \in S', \tag{A.25}$$

$$x_d^t \in \{0,1\} \qquad \forall t \in T, \forall d \in D, \tag{A.26}$$

$$b_{il} \in \{0,1\} \qquad \forall i \in I, l \in L, \tag{A.27}$$

$$y_{sl} \geq 0 \qquad \forall s \in S_l', l \ in L, \tag{A.28}$$

$$z_{sl} \geq 0 \qquad \forall s \in S_l', l \in L, \tag{A.29}$$

$$w_{sl} \geq 0 \qquad \forall s \in S_l', l \in L \tag{A.30}$$

$$o_l \geq 0 \qquad \forall l \in L, \tag{A.31}$$

$$h_{sl}^{travel}, h_{sl}^{dwell} \geq 0 \qquad \forall s \in S_l', l \in L, \tag{A.32}$$

$$DOD_{il} \geq 0 \qquad \forall i \in I, l \in L, \tag{A.33}$$

$$SOC_{il}^{avg} \geq 0 \qquad \forall i \in I, l \in L. \tag{A.34}$$

References

Abdelwahed, A., van den Berg, P.L., Brandt, T., Collins, J., Ketter, W., 2020. Evaluating and optimizing opportunity fast-charging schedules in transit battery electric bus networks. Transp. Sci. 54 (6), 1601–1615.

Adler, J.D., Mirchandani, P.B., 2014. Online routing and battery reservations for electric vehicles with swappable batteries. Transp. Res. B 70, 285–302.

An, K., 2020. Battery electric bus infrastructure planning under demand uncertainty. Transp. Res. C 111, 572–587.

Arslan, O., Yıldız, B., Karaşan, O.E., 2015. Minimum cost path problem for plug-in hybrid electric vehicles. Transp. Res. E 80, 123–141.

Augé, O., 2015. Keynote 2: TOSA concept: A full electric large capacity urban bus system. In: 2015 17th European Conference on Power Electronics and Applications (EPE'15 ECCE-Europe). IEEE, p. 1.

Barco, J., Guerra, A., Muñoz, L., Quijano, N., 2017. Optimal routing and scheduling of charge for electric vehicles: A case study. Math. Probl. Eng. 2017.

Barré, A., Deguilhem, B., Grolleau, S., Gérard, M., Suard, F., Riu, D., 2013. A review on lithium-ion battery ageing mechanisms and estimations for automotive applications. J. Power Sources 241, 680–689.

Bekli, S., Boyacı, B., Zografos, K.G., 2021. Enhancing the performance of one-way electric carsharing systems through the optimum deployment of fast chargers. Transp. Res. B 152, 118–139.

Brandstätter, G., Kahr, M., Leitner, M., 2017. Determining optimal locations for charging stations of electric car-sharing systems under stochastic demand. Transp. Res. B 104, 17–35.

Chen, Z., Liu, W., Yin, Y., 2017. Deployment of stationary and dynamic charging infrastructure for electric vehicles along traffic corridors. Transp. Res. C 77, 185–206.

Chen, Z., Yin, Y., Song, Z., 2018. A cost-competitiveness analysis of charging infrastructure for electric bus operations. Transp. Res. C 93, 351–366.

Edenhofer, O., 2015. Climate Change 2014: Mitigation of Climate Change. Vol. 3, Cambridge University Press.

Erdinc, O., Vural, B., Uzunoglu, M., 2009. A dynamic lithium-ion battery model considering the effects of temperature and capacity fading. In: 2009 International Conference on Clean Electrical Power. IEEE, pp. 383–386.

He, F., Wu, D., Yin, Y., Guan, Y., 2013. Optimal deployment of public charging stations for plug-in hybrid electric vehicles. Transp. Res. B 47, 87–101.

Hoke, A., Brissette, A., Maksimović, D., Pratt, A., Smith, K., 2011. Electric vehicle charge optimization including effects of lithium-ion battery degradation. In: 2011 IEEE Vehicle Power and Propulsion Conference. IEEE, pp. 1–8.

Hua, Y., Zhao, D., Wang, X., Li, X., 2019. Joint infrastructure planning and fleet management for one-way electric car sharing under time-varying uncertain demand. Transp. Res. B 128, 185–206.

Infrastructure, A.E.C., 2015. ABB introduces automated fast chargers for electric city busses enabling zero emission public transportation in cities. https://library.e.abb.com/public/01a9347a808e4cefa6e4534ee63a2876/4EVC500301-LFEN_BusCharger.pdf/, [Online; accessed 8-July-2022].

Kınay, O.B., Gzara, F., Alumur, S.A., 2021. Full cover charging station location problem with routing. Transp. Res. B 144, 1–22.
Kunith, A., Mendelevitch, R., Goehlich, D., 2017. Electrification of a city bus network—An optimization model for cost-effective placing of charging infrastructure and battery sizing of fast-charging electric bus systems. Int. J. Sustain. Transp. 11 (10), 707–720.
Lajunen, A., 2014a. Energy consumption and cost-benefit analysis of hybrid and electric city buses. Transp. Res. C 38, 1–15.
Lajunen, A., 2014b. Energy consumption and cost-benefit analysis of hybrid and electric city buses. Transp. Res. C 38, 1–15.
Lee, C., Han, J., 2017. Benders-and-Price approach for electric vehicle charging station location problem under probabilistic travel range. Transp. Res. B 106, 130–152.
Li, J.-Q., 2016. Battery-electric transit bus developments and operations: A review. Int. J. Sustain. Transp. 10 (3), 157–169.
Lin, Y., Zhang, K., Shen, Z.-J.M., Ye, B., Miao, L., 2019. Multistage large-scale charging station planning for electric buses considering transportation network and power grid. Transp. Res. C 107, 423–443.
Marano, V., Onori, S., Guezennec, Y., Rizzoni, G., Madella, N., 2009. Lithium-ion batteries life estimation for plug-in hybrid electric vehicles. In: Vehicle Power and Propulsion Conference. IEEE, pp. 536–543.
Markel, T., Smith, K., Pesaran, A.A., 2009. Improving petroleum displacement potential of PHEVs using enhanced charging scenarios. In: Electric and Hybrid Vehicles Power Sources, Models, Sustainability, Infrastructure and the Market. Elsevier, pp. 211–225.
Mohamed, M., Farag, H., El-Taweel, N., Ferguson, M., 2017. Simulation of electric buses on a full transit network: Operational feasibility and grid impact analysis. Electr. Power Syst. Res. 142, 163–175.
Ngatchou, P., Zarei, A., El-Sharkawi, A., 2005. Pareto multi objective optimization. In: Proceedings of the 13th International Conference on, Intelligent Systems Application to Power Systems. IEEE, pp. 84–91.
Paul, T., Yamada, H., 2014. Operation and charging scheduling of electric buses in a city bus route network. In: Intelligent Transportation Systems (ITSC), 2014 IEEE 17th International Conference on. IEEE, pp. 2780–2786.
Pelletier, S., Jabali, O., Laporte, G., 2018. Charge scheduling for electric freight vehicles. Transp. Res. B 115, 246–269.
Pelletier, S., Jabali, O., Laporte, G., Veneroni, M., 2017. Battery degradation and behaviour for electric vehicles: Review and numerical analyses of several models. Transp. Res. B 103, 158–187.
Pelletier, S., Jabali, O., Mendoza, J.E., Laporte, G., 2019. The electric bus fleet transition problem. Transp. Res. C 109, 174–193.
Perrotta, D., Macedo, J.L., Rossetti, R.J., de Sousa, J.F., Kokkinogenis, Z., Ribeiro, B., Afonso, J.L., 2014. Route planning for electric buses: a case study in Oporto. Procedia-Social Behav. Sci. 111, 1004–1014.
Pesaran, A.A., Markel, T., Tataria, H.S., Howell, D., 2009. Battery requirements for plug-in hybrid electric vehicles–analysis and rationale. Tech. rep., National Renewable Energy Lab.(NREL), Golden, CO (United States).
Pihlatie, M., Paakkinen, M., 2017. Requirements and technology for electric bus fast charging infrastructure. In: International Conference Electric Mobility and Public Transport. VTT Research.
Quarles, N., Kockelman, K.M., Mohamed, M., 2020. Costs and benefits of electrifying and automating bus transit fleets. Sustainability 12 (10), 3977.
Rios, M., Munoz, L., Zambrano, S., Albarracin, A., 2014. Load profile for a bus rapid transit flash station of full-electric buses. In: IEEE PES Innovative Smart Grid Technologies, Europe. IEEE, pp. 1–6.
Rogge, M., Wollny, S., Sauer, D.U., 2015. Fast charging battery buses for the electrification of urban public transport-a feasibility study focusing on charging infrastructure and energy storage requirements. Energies 8 (5), 4587–4606.
Scarinci, R., Zanarini, A., Bierlaire, M., 2019. Electrification of urban mobility: The case of catenary-free buses. Transp. Policy 80, 39–48.
Schoch, J., Gaerttner, J., Schuller, A., Setzer, T., 2018. Enhancing electric vehicle sustainability through battery life optimal charging. Transp. Res. B 112, 1–18.
Sebastiani, M.T., Lüders, R., Fonseca, K.V.O., 2016. Evaluating electric bus operation for a real-world BRT public transportation using simulation optimization. IEEE Trans. Intell. Transp. Syst. 17 (10), 2777–2786.
Shen, Z.-J.M., Feng, B., Mao, C., Ran, L., 2019. Optimization models for electric vehicle service operations: A literature review. Transp. Res. B 128, 462–477.
Sinhuber, P., Rohlfs, W., Sauer, D.U., 2012. Study on power and energy demand for sizing the energy storage systems for electrified local public transport buses. In: Vehicle Power and Propulsion Conference (VPPC). IEEE, pp. 315–320.
Smith, K., Markel, T., Kim, G.-H., Pesaran, A., 2010. Design of electric drive vehicle batteries for long life and low cost: Robustness to geographic and consumer-usage variation (presentation). Tech. rep., National Renewable Energy Laboratory (NREL), Golden, CO..
Tomaszewska, A., Chu, Z., Feng, X., O'Kane, S., Liu, X., Chen, J., Ji, C., Endler, E., Li, R., Liu, L., et al., 2019. Lithium-ion battery fast charging: a review. ETransportation 1, 100011.
Waterstaat, M.v.I.e., 2016. Dutch public transport switches to 100 percent emissions-free buses. URL https://www.government.nl/latest/news/2016/04/15/dutch-public-transport-switches-to-100-percent-emissions-free-buses.
World, E., 2008. Beijing readies electric buses for summer olympics.
Xu, B., 2013. Degradation-limiting optimization of battery energy storage systems operation. (Master's thesis). Eidgenössische Technische Hochschule, Zürich, Switzerland.
Xu, M., Meng, Q., Liu, K., Yamamoto, T., 2017. Joint charging mode and location choice model for battery electric vehicle users. Transp. Res. B 103, 68–86.
Xu, B., Oudalov, A., Ulbig, A., Andersson, G., Kirschen, D.S., 2016. Modeling of lithium-ion battery degradation for cell life assessment. IEEE Trans. Smart Grid 9 (2), 1131–1140.
Xu, M., Wu, T., Tan, Z., 2021. Electric vehicle fleet size for carsharing services considering on-demand charging strategy and battery degradation. Transp. Res. C 127, 103146.
Xylia, M., Leduc, S., Patrizio, P., Kraxner, F., Silveira, S., 2017. Locating charging infrastructure for electric buses in Stockholm. Transp. Res. C 78, 183–200.
Yıldırım, Ş., Yıldız, B., 2021. Electric bus fleet composition and scheduling. Transp. Res. C 129, 103197.
Yıldız, B., Olcaytu, E., Şen, A., 2019. The urban recharging infrastructure design problem with stochastic demands and capacitated charging stations. Transp. Res. B 119, 22–44.
Zanarini, A., Poland, J., Ferreau, H.J., Mercangoez, M., Bierlaire, M., Scarinci, R., Lurkin, V., Horsky, M., Azadeh, S.S., Maknoon, Y., et al., 2020. Method and device for determining a configuration for deployment of a public transportation system. US Patent App. 16/542, 836.
Zhang, A., Kang, J.E., Kwon, C., 2017. Incorporating demand dynamics in multi-period capacitated fast-charging location planning for electric vehicles. Transp. Res. B 103, 5–29.